1998

Radio/x-ray luminosity relation for advection-dominated accretion: implications for emission line galaxies and the x-ray background

Stephen P. Boughn
Haverford College, sboughn@haverford.edu

Insu Yi

THE ASTROPHYSICAL JOURNAL, 499:198–204, 1998 May 20

RADIO/X-RAY LUMINOSITY RELATION FOR ADVECTION-DOMINATED ACCRETION: IMPLICATIONS FOR EMISSION-LINE GALAXIES AND THE X-RAY BACKGROUND

INSU YI[1] AND STEPHEN P. BOUGHN[1,2]

Received 1997 September 15; accepted 1998 January 1

ABSTRACT

Recent studies of the cosmic X-ray background (XRB) have suggested the possible existence of a population of relatively faint sources with hard X-ray spectra; however, the emission mechanism remains unclear. If the hard X-ray emission is from the radiatively inefficient, advection-dominated accretion flows (ADAFs) around massive black holes in galactic nuclei, X-ray luminosity and radio luminosity satisfy the approximate relation $L_R \sim 7 \times 10^{35}(\nu/15\ \mathrm{GHz})^{7/5}(M/10^7\ M_\odot)(L_X/10^{40}\ \mathrm{ergs\ s^{-1}})^{1/10}\ \mathrm{ergs\ s^{-1}}$, where $L_R = \nu L_\nu$ is the radio luminosity at frequency ν, M is the mass of the accreting black hole, and $10^{40} \lesssim L_X \lesssim 10^{42}$ ergs s^{-1} is the 2–10 keV X-ray luminosity. These sources are characterized by inverted radio spectra $I_\nu \propto \nu^{2/5}$. For example, an ADAF X-ray source with luminosity $L_X \sim 10^{41}$ ergs s^{-1} has a nuclear radio luminosity of $\sim 4 \times 10^{36}(M/3 \times 10^7\ M_\odot)$ ergs s^{-1} at ~ 20 GHz, and if it is at a distance of $\sim 10(M/3 \times 10^7\ M_\odot)^{1/2}$ Mpc, it would be detected as a ~ 1 mJy point radio source. High-frequency (~ 20 GHz), high angular resolution radio observations provide an important test of the ADAF emission mechanism. Since L_R depends strongly on black hole mass and only weakly on X-ray luminosity, the successful measurement of nuclear radio emission could provide an estimate of black hole mass. Because the X-ray spectra produced by ADAFs are relatively hard, sources of this emission are natural candidates for contributing to the hard (>2 keV) background.

Subject headings: accretion, accretion disks — black hole physics — galaxies: nuclei — radiation mechanisms: nonthermal — radio continuum: galaxies — X-rays: galaxies

1. INTRODUCTION

Recent progress in the study of the cosmic X-ray background (XRB) has shown that discrete sources probably account for the entire XRB (e.g., Hasinger et al. 1993). Although broad-line QSOs account for more than half of, and perhaps the entire, 0.5–2.0 keV XRB (Boyle et al. 1994; Georgantopoulos et al. 1996; Hasinger et al. 1997; Schmidt et al. 1998), at higher energies (>2 keV), the QSO spectrum with an energy spectral index of $\alpha_X \sim 1.2$ is too soft to account for the XRB for which $\alpha_X \sim 0.4$ (Gendreau et al. 1995). Moreover, QSOs are significantly more clustered than the diffuse component of the XRB (Georgantopoulos et al. 1993; Soltan & Hasinger 1994). The emission from Seyfert nuclei is somewhat harder, $\alpha_X \sim 0.7$, but is still too soft to account for the XRB unless there is a large population of highly absorbed Seyfert galaxies ($N_H > 10^{22}$ cm^{-3}). Comastri et al. (1995) have successfully modeled the amplitude and general shape of the XRB spectrum with a unified active galactic nuclei (AGNs) model that includes such sources; however, the characteristic reflection feature in the obscured Seyfert spectrum (e.g., Ghisellini, Haardt, & Matt 1994) has not been observed in the XRB (Gendreau et al. 1995). X-ray spectra of starburst galaxies are too soft and their luminosities too low to make a significant contribution (Della-Ceca et al. 1996).

One possible resolution to this problem would be a population of "X-ray galaxies" that are relatively faint but have intrinsically hard spectra. This possibility has become especially interesting since the recent discovery of narrow emission line galaxies with nuclear X-ray luminosities of $\sim 10^{41}$–10^{43} ergs s^{-1} (Georgantopoulos et al. 1996; Griffiths et al. 1996). Such sources are ~ 100 times more luminous than "normal" field galaxies (Fabbiano 1989), yet fainter than typical AGNs. If a significant fraction of narrow emission line galaxies are similar X-ray sources, then they could make a substantial contribution to the XRB. The emission mechanism in these sources is still unknown.

There is already evidence that X-ray emission from faint galaxies contributes significantly to the XRB. Almaini et al. (1997) cross-correlated unidentified X-ray sources from three deep *ROSAT* fields and optically faint galaxies and concluded that galaxies with *B*-band magnitudes less than 23 account for $\sim 20\%$ of all X-ray sources to a flux limit of 4×10^{-15} ergs s^{-1} cm^{-2} in the 0.5–2 keV range. They also found that the X-ray luminosity of these faint galaxies evolves as $(1+z)^{3.22 \pm 0.98}$, with a comoving emissivity at the present epoch of $j_0 \approx (3.02 \pm 0.23) \times 10^{38}\ h$ ergs s^{-1} Mpc^{-3} in the *ROSAT* band. If integrated to $z_c = 2$, $80\% \pm 20\%$ of the 0.5–2 keV XRB and $40\% \pm 10\%$ of the total XRB are accounted for (see § 4 below). This tentative conclusion emphasizes the need for a better understanding of the X-ray emission mechanism from faint sources.

If nuclear emission in X-ray galaxies were to arise from accretion disks around massive black holes, i.e., the standard AGN mechanism, and if the central black hole masses are similar to those of AGNs, then the mass-accretion rates would be orders of magnitude lower than those for typical AGNs (e.g., Frank, King, & Raine 1992). On the other hand, the relatively low X-ray luminosity could be due to the low radiative efficiency expected in hot advection-dominated accretion flows (ADAFs) (e.g., Rees et al. 1982; Narayan & Yi 1995 and references therein). In the latter case, the accretion rates could be similar to those of AGNs (e.g., Yi 1996). This possibility is especially interesting since X-ray emission spectra from ADAFs are intrinsically hard enough to account for the XRB (Di Matteo & Fabian 1997). We

[1] Institute for Advanced Study, Olden Lane, Princeton, NJ 08540; yi@sns.ias.edu.
[2] Department of Astronomy, Haverford College, Haverford, PA 19041; sboughn@haverford.edu.

suggest that these two possible X-ray emission mechanisms can be distinguished by the radio emission that is inherent in ADAFs. The radio detection of such sources at distances of $\lesssim 10$ Mpc would have important implications for the masses of black holes and possibly for the nature of the XRB.

We adopt the following dimensionless variables: mass of the black hole $m = M/M_\odot$; cylindrical radius from the black hole $r = R/R_s$ ($R_s = 2GM/c^2 = 2.95 \times 10^5 m$ cm is the Schwarzschild radius); and mass-accretion rate $\dot{m} = \dot{M}/\dot{M}_{\rm Edd}$, where $\dot{M}_{\rm Edd} = L_{\rm Edd}/\eta_{\rm eff} c^2 = 1.39 \times 10^{18}$ mg s^{-1} is the Eddington accretion rate assuming a 10% efficiency, $\eta_{\rm eff} = 0.1$.

2. RADIO/X-RAY LUMINOSITY RELATION

2.1. *ADAFs in Galactic Nuclei*

When the density of the accretion flow is sufficiently low, the radiative cooling rate becomes smaller than the viscous heating rate. As a result, the dissipated accretion energy is not efficiently radiated away but kept as internal heat and advected inward with the accreted plasma (Rees et al. 1982; Narayan & Yi 1995 and references therein). In ADAFs, ions reach a very high temperature (close to the virial temperature), the energy transfer from ions to electrons becomes slow, and the radiative cooling by electrons remains very inefficient. Suppose ions are heated by viscous dissipation at a rate of q_+ per unit volume and that viscous heating is characterized by the usual viscosity parameter α. We assume $\alpha = 0.3$ (e.g., Frank et al. 1992; Narayan & Yi 1995); however, the following results are not very sensitive to α unless $\alpha \ll 0.1$. The ADAF emission depends on the ratio $\dot{M}/\alpha$, so solutions with different α-values are equivalent if $\dot{M}$ is appropriately rescaled. The viscous heating rate is balanced by the energy advection rate $q_{\rm adv}$ per unit volume and the rate of energy transfer to electrons q_{e+} per unit volume:

$$q_+ = q_{\rm adv} + q_{e+} \ . \tag{2.1}$$

When the radiative cooling is inefficient, the accreted plasma becomes hot and the internal (thermal and magnetic) pressure becomes comparable to the kinetic pressure. The dependence of emission on the magnetic field is more important (e.g., Rees et al. 1982; Narayan & Yi 1995). We adopt the equipartition condition that the magnetic pressure is equal to half the total internal pressure. Then the magnetic field in the ADAF is (Narayan & Yi 1995)

$$B \approx 1.1 \times 10^4 m_7^{-1/2} \dot{m}_{-3}^{1/2} r^{-5/4} \ {\rm G} \ , \tag{2.2}$$

where $m_7 = m/10^7$ and $\dot{m}_{-3} = \dot{m}/10^{-3}$. Hot electrons in magnetic fields radiate through the emission of synchrotron photons, the Comptonization of synchrotron photons, and bremsstrahlung, for which we take $q_{\rm sync}$, $q_{\rm C}$, and $q_{\rm br}$ as the corresponding rates per unit volume. The synchrotron emission gives rise to radio and submillimeter emission, the Comptonization of synchrotron photons produces optical and X-ray photons, and bremsstrahlung contributes only to the X-ray luminosity. Balancing the heating rate q_{e+} and the total cooling rate, i.e.,

$$q_{e+} = q_{\rm sync} + q_{\rm C} + q_{\rm br} \ , \tag{2.3}$$

and simultaneously solving equation (2.1), we self-consistently determine the electron temperature of the ADAF and radiative luminosities in the radio and X-ray (for details, see Narayan & Yi 1995). ADAFs exist for mass-accretion rates $\dot{m} < \dot{m}_{\rm crit} \approx 0.3\alpha^2 \sim 10^{-1.6}$ (Rees et al. 1982; Narayan & Yi 1995). The bolometric luminosity of the ADAF, $L_{\rm ADAF}$, is roughly given by $L_{\rm ADAF} \sim \eta L_E$, where $\eta \sim 10\dot{m}^2$ (Narayan & Yi 1995). We assume that an ADAF extends from the inner radius of $r_{\rm min} = 3$ and take the outer extent of the flow as $r_{\rm max} \gg r_{\rm min}$. In this regime, the results depend very weakly on $r_{\rm max}$.

2.2. *Radio/X-Ray Luminosity Relation from ADAFs*

Figure 1 shows radio luminosity νL_ν at four different frequencies (1.4, 5, 15, and 20 GHz) as a function of X-ray luminosity in two X-ray bands (0.5–2 and 2–10 keV). For each black hole mass, luminosities are calculated for $\dot{m} = 10^{-4}$–$10^{-1.6}$. The lower value of $\dot{m}$ roughly corresponds to the limit above which the electron heating is dominated by the Coulomb coupling (e.g., Mahadevan 1996). The upper limit, in principle, corresponds to $\dot{m}_{\rm crit}$ for $\alpha = 0.3$. We note, however, that the exact physical nature of the ADAF for $\dot{m} \sim \dot{m}_{\rm crit}$ is poorly understood. Therefore, luminosity curves for $\dot{m} \sim \dot{m}_{\rm crit}$ (the far right-hand part of the curves in Fig. 1; see also Fig. 2) are suspect (Narayan & Yi 1995). In each panel, from bottom to top, the black hole mass increases as 3×10^6, 10^7, 3×10^7, 10^8, 3×10^8 $M_\odot$. The curves are steeper at low luminosities and flatter at high luminosities. This trend is caused by the change in the dominant X-ray emission mechanism. At lower luminosities, the X-ray luminosity is mainly contributed by bremsstrahlung, whereas at high luminosities Compton scattering becomes important (e.g., Rees et al. 1982; Narayan & Yi 1995).

The results shown in Figure 1 can be qualitatively understood as follows. Optically thin synchrotron emission extends to the self-absorption frequency, ν_s, at which the Rayleigh-Jeans blackbody emission equals the optically thin synchrotron emission. Therefore, the radio luminosity at frequency ν comes from a radial region where $\nu \approx \nu_s(R)$, i.e., $L_\nu(\nu) \approx (8\pi^2 k/c^2) R^2 T_e \nu^2$, where T_e is the electron temperature and

$$\nu_s(r) \approx 9 \times 10^{11} m_7^{-1/2} \dot{m}_{-3}^{1/2} T_{e9}^2 r^{-5/4} \ {\rm Hz} \tag{2.4}$$

(Narayan & Yi 1995; Mahadevan 1996). In terms of the ADAF parameters (Rees et al. 1982; Narayan & Yi 1995; Mahadevan 1996)

$$L_R(\nu) \equiv \nu L_\nu^{\rm sync} \approx 2 \times 10^{32} x_{M3}^{8/5} m_7^{6/5} \dot{m}_{-3}^{4/5} T_{e9}^{21/5} \nu_{10}^{7/5} \ {\rm ergs \ s^{-1}} \ , \tag{2.5}$$

where $\nu_{10} = \nu/10^{10}$ Hz and $x_{M3} = x_M/10^3 \sim 1$ is the dimensionless synchrotron self-absorption frequency (Narayan & Yi 1995). Both T_e and x_{M3} vary slowly with R in the inner regions of the ADAF (Narayan & Yi 1995; Narayan, Yi, & Mahadevan 1995). The highest radio emission frequency, $\nu_{\rm max}$, arises from the innermost radius of the accretion flow $r_{\rm min} \sim 3$; i.e.,

$$\nu_{\rm max} \approx 2 \times 10^{11} m_7^{-1/2} \dot{m}_{-3}^{1/2} T_{e9}^2 \ {\rm Hz} \ , \tag{2.6}$$

and the lowest radio emission frequency is expected from the outermost radius of ADAF $r_{\rm max} \gg r_{\rm min}$; i.e.,

$$\nu_{\rm min} = \nu_{\rm max} (r_{\rm max}/r_{\rm min})^{-5/4} \ . \tag{2.7}$$

The inverted power-law radio spectrum (eq. [2.5]) is the characteristic radio emission spectrum from an optically thin ADAF. This spectrum agrees with those for the Galactic center source Sgr A* shown by Narayan & Yi (1995),

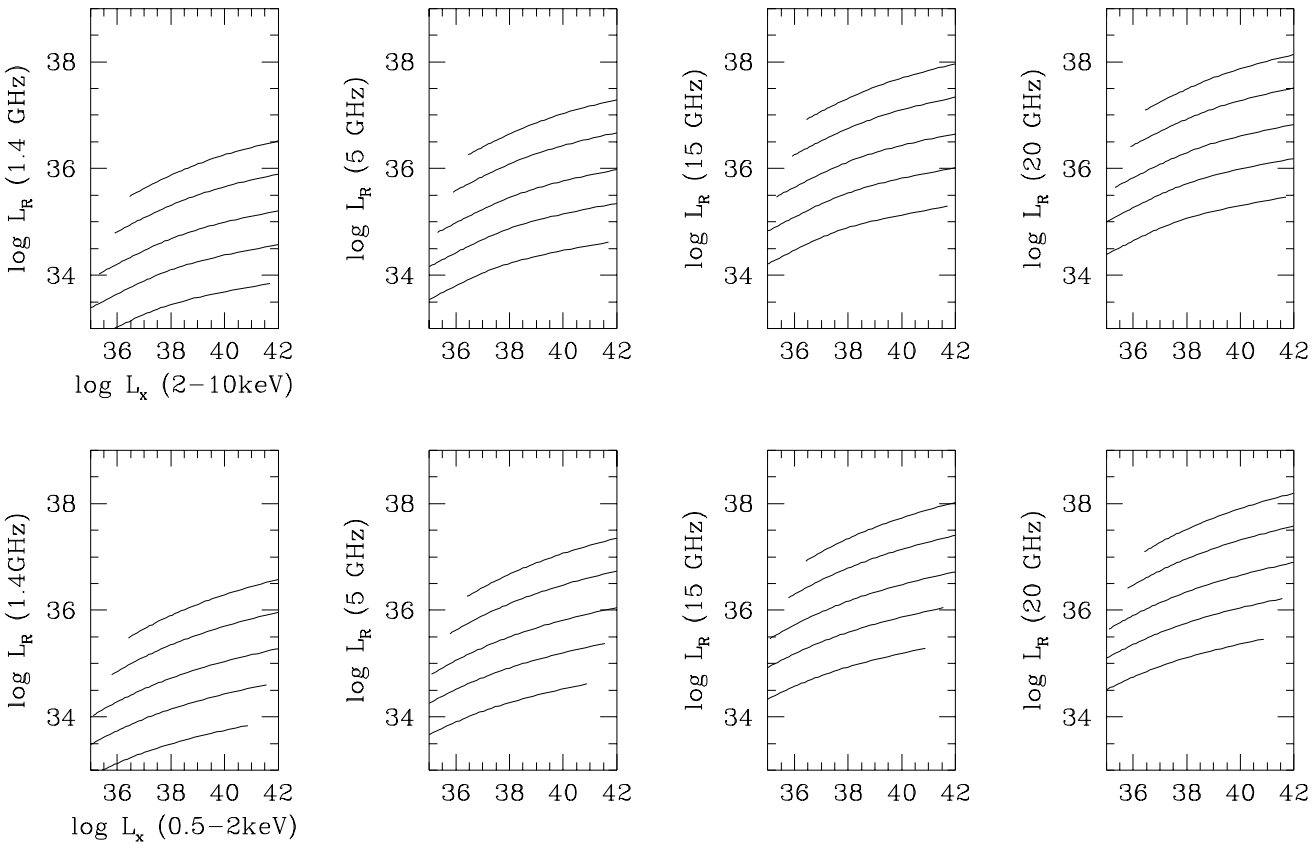

FIG. 1.—X-ray luminosity vs. radio luminosity for four black hole masses in ergs s^{-1} units. In each panel, the black hole mass increases as 3×10^6, 10^7, 3×10^7, 10^8, and 3×10^8 solar masses from bottom to top curves. In the top panels, the X-ray luminosity is for the 2–10 keV band, and in the bottom panels, the X-ray luminosity refers to the 0.5–2 keV range. From left to right, the radio frequency increases from 1.4 to 20 GHz.

Narayan et al. (1997), and Manmoto, Mineshige, & Kusunose (1997). Similar inverted spectra with sharp submillimeter cutoffs could be obtained by synchrotron emission from nearly monoenergetic, relativistic electrons with self-absorption. In the case of Sgr A*, however, such an emission mechanism cannot self-consistently account for X-ray emission (e.g., Beckert & Duschl 1997).

When the accretion rate $\dot{m}$ is substantially lower than $\dot{m}_{\rm crit}$, the X-ray emission comes mainly from the bremsstrahlung emission (Narayan & Yi 1995). Compton scattering contributes significantly when the mass-accretion rate approaches the critical rate at which $\dot{m}_{\rm crit}$ is approximately a few times 10^{-2}. The X-ray luminosity due to the bremsstrahlung emission is

$$L_{\rm X}(\nu) \equiv \nu L_\nu^{\rm brem} \approx 2 \times 10^{39} m_7 \dot{m}_{-3}^2 T_{e9}^{-3/2} \nu_{18} \times \exp(-4 \times 10^{-2} \nu_{18}/T_{e9}) \text{ ergs s}^{-1}, \quad (2.8)$$

where $\nu_{18} = \nu/10^{18}$ Hz, and we have assumed that kT_e is smaller than the electron rest energy. The Compton luminosity results from the upscattering of the synchrotron photons and can be approximated by

$$\nu L_\nu^{\rm Compt} \approx \nu_{\rm max}^{\alpha_c} L_\nu^{\rm sync}(\nu_{\rm max}) \nu^{1-\alpha_c} \text{ ergs s}^{-1}, \quad (2.9)$$

where the index of the Compton-scattering spectrum $\alpha_c = -\ln \tau_{\rm es}/\ln A$, the electron-scattering depth $\tau_{\rm es} \approx 5 \times 10^{-2} \dot{m}_{-3}$, and the scattering amplification factor $A \approx 1 + 0.7 T_{e9}$ (Narayan & Yi 1995; Mahadevan 1996 and references therein). Compton scattering is an important mechanism for X-ray emission for $\dot{m} \gtrsim 10^{-3}$, while bremsstrahlung dominates for $\dot{m} \lesssim 10^{-3}$.

In the bremsstrahlung-dominated regime, $L_{\rm X} \propto m\dot{m}^2$ and $L_R \propto m^{8/5}\dot{m}^{6/5}$. These simple scalings are valid when the X-ray photon energy is sufficiently smaller than kT_e (cf. eq. [2.8]). T_e is approximately independent of $\dot{m}$ and m, and $x_M \propto (\dot{m}m)^{1/4}$ (Mahadevan 1996). Then, since $\dot{m} \propto (L_{\rm X}/m)^{1/2}$, we immediately arrive at $L_R \propto m L_{\rm X}^{3/5}$, which qualitatively accounts for the low X-ray luminosity, steeper parts of the curves in Figure 1. On the other hand, when $\dot{m} \gtrsim 10^{-3}$, the X-ray photons in the 0.5–10 keV range are contributed primarily by Compton–up-scattered synchrotron photons. The luminosity of synchrotron photons upscattered N times into the X-ray range is roughly $\propto L(\nu = \nu_{\rm max})(A\tau_{\rm es})^N \propto \dot{m}^{N+1}$. For Compton-scattered photons at energies $\sim$2–10 keV, $N > 2$. Therefore, $L_{\rm X} \propto \dot{m}^{N+1}$, and the dependence on $\dot{m}$ is stronger than in the bremsstrahlung-dominated regime. Thus $\dot{m} \propto L_{\rm X}^{1/(N+1)}$ and $L_R \propto L_{\rm X}^{6/5(N+1)}$, which accounts for the flatter parts of the curves in Figure 1. While this argument describes the qualitative shape of the luminosity relations, more detailed calculations give an even smaller slope at high $L_{\rm X}$.

The typical radio spectrum peaks at frequencies greater than 20 GHz (eqs. [2.5], and [2.6]), so the radio to X-ray luminosity ratio increases with radio frequency. The radio/X-ray luminosity relation shown in Figure 1 can be approximated by

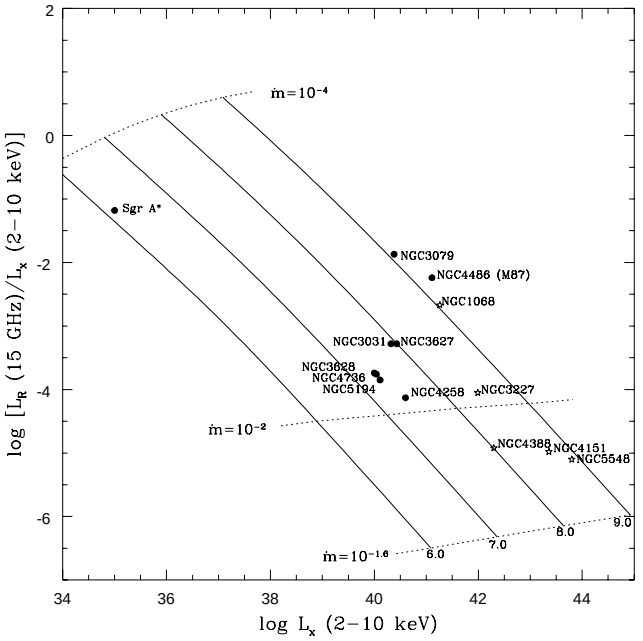

FIG. 2.—Ratios of 15 GHz luminosity to 2–10 keV luminosity for eight LINERs (NGC 3031, 3079, 3627, 3628, 4258, 4486, 4736, and 5194), the Galactic center radio source Sgr A*, and five Seyfert galaxies (NGC 1068, 3227, 4151, 5548, and 4388). Because of finite angular resolution in the radio, the ratios should be considered as upper limits. The theoretical curves are (*from bottom to top*) for black hole masses log $M/M_\odot$ of 6.0–9.0 as marked with the numbers. The X-ray fluxes are from Serlemitsos, Ptak, & Yaqoob (1997); Brinkmann, Siebert, & Boller (1994); Makishima et al. (1994); Fabbiano, Kim, & Trinchieri (1992); Reynolds et al. (1996); Smith & Done (1996); and Papadakis & McHardy (1995). The radio fluxes are from Turner & Ho (1994); Carral, Turner, & Ho (1990); Saikia et al. (1994); Spencer & Junor (1986); Moellenbrock et al. (1996); and Gallimore et al. (1996). The dotted lines indicate the luminosity ratios for given $\dot{m} = 10^{-4}, 10^{-2}, 2.5 \times 10^{-2}$.

$$L_R = \nu L_\nu \approx 7 \times 10^{35} m_7 L_{x,40}^{1/10} (\nu/15\ \mathrm{GHz})^{7/5}\ \mathrm{ergs\ s^{-1}}\ , \tag{2.10}$$

where $L_{X,40} = L_X/10^{40}$ ergs s^{-1} is the X-ray luminosity in the 2–10 keV band and we have approximated the exponents to the closest simple fractions. Despite the change in slope of the luminosity curves in Figure 1, this simple radio/X-ray luminosity relation is valid to within a factor of 2 in the luminosity range 10^{40} ergs s$^{-1} \lesssim L_X \lesssim 10^{42}$ ergs s^{-1}. Since L_R is strongly dependent on m and only mildly dependent on L_X, the observed radio luminosity provides an important constraint on the mass of the central black hole. On the other hand, the inverted radio spectrum provides an important signature of the ADAF mechanism and indicates the importance of high-frequency ($\nu \gtrsim 5$ GHz) observations.

2.3. *Accretion Flows for High Mass-Accretion Rates*

When the accretion rate becomes higher than $\dot{m}_{\rm crit}$, the low radiative efficiency ADAFs no longer exist (Narayan & Yi 1995). These flows differ from ADAFs mainly because of their high radiative efficiency. If the accretion flows of the low-luminosity galactic nuclei are similar to those of high-luminosity Seyferts and QSOs (e.g., Frank et al. 1992), the high efficiency implies a very low mass-accretion rate. For instance, $m \sim 10^7$ with $L_X \sim 10^{41}$ ergs s^{-1} requires $\dot{m} \sim 10^{-4}$, whereas the ADAFs would require an $\dot{m}$ roughly 2 orders of magnitude higher. Since the high-efficiency accretion flows are most likely to occur in the form of the thin disk (e.g., Frank et al. 1992), a clear correlation between the radio emission and the X-ray emission comparable to equation (2.10) is not expected.

3. NEARBY CANDIDATES FOR ADAF X-RAY SOURCES

Radio emission provides a characteristic signature for ADAF sources; however, the fluxes are relatively low and undetectable for distant sources. For example, an ADAF source with X-ray luminosity $L_X \sim 10^{41}$ ergs s^{-1} and mass $M \sim 3 \times 10^7\ M_\odot$ at $z = 1$ has a 20 GHz flux of $\sim 10^{-8}$ Jy. In addition, resolving small nuclear regions at this distance is problematic. On the other hand, if ADAF sources are responsible for a significant fraction of the XRB, then their required number density, $\sim 3 \times 10^{-3}$ Mpc^{-3} (see § 4), is a significant fraction of the density of field galaxies and they should be easily observable in the local universe. If an X-ray–bright galaxy contains an ADAF with $L_X \sim 10^{41}$ ergs s^{-1}, the 20 GHz radio luminosity is expected to be $\sim 4 \times 10^{36} (M/3 \times 10^7\ M_\odot)$ ergs s^{-1}. Such a galaxy would be detected as a $\gtrsim 1$ mJy radio source out to a distance of $\sim 10 (M/3 \times 10^7\ M_\odot)^{1/2}$ Mpc. High-resolution 10 and 20 GHz observations of nearby sources would test the prediction that the radio spectra are inverted, and careful X-ray observations (e.g., by *ASCA*, *AXAF*, and/or *XMM*) would test the predicted hardness of the X-ray spectrum. In Figure 3, we show an example of the broadband spectrum from an ADAF source with a black hole mass of $3 \times 10^7\ M_\odot$ at a distance of 10 Mpc. In this particular example, the radio flux at 15 GHz is ~ 1 mJy. The expected X-ray spectrum is characteristically "flat" (e.g., Lasota et al. 1996) with an energy spectral index $\alpha_X \gtrsim 0$. In fact, a large effort to characterize the spectrum of low ionization nuclear emission regions (LINERs) and low-luminosity AGNs at many wavelengths is already underway (L. C. Ho 1997, private communication) and should provide a test of the general characteristics of the ADAF mechanism in these sources. Recently, Falcke, Wilson, & Ho (1997) reported the results of their 15 GHz radio survey of 48 nearby LINERs optically observed by Ho, Filippenko, & Sargent (1995).

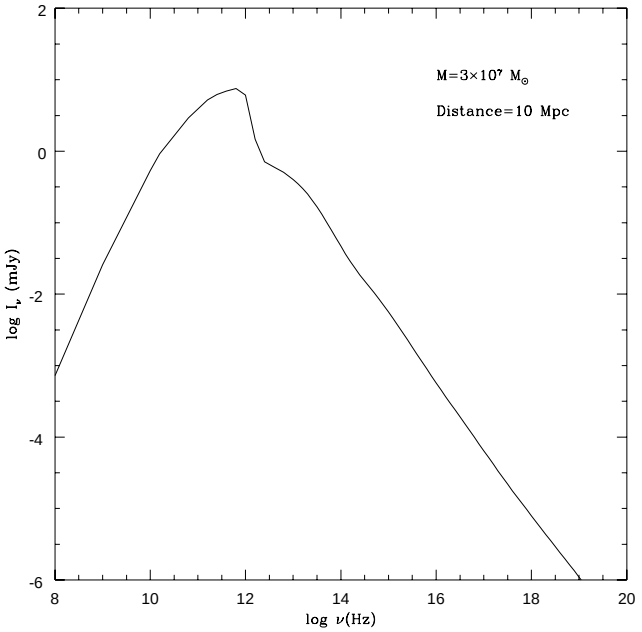

FIG. 3.—Example of the broadband spectrum from an ADAF. This example assumes a source with $M = 3 \times 10^7\ M_\odot$ at a distance of 10 Mpc with the radio flux of ~ 1 mJy at 15 GHz.

Nuclear radio emission above the 1 mJy flux limit was detected in 25% of the LINERs. The observed luminosities are the right order of magnitude, but further observations at different radio frequencies would be very useful.

3.1. *Galactic Center Source Sgr A**

Sgr A* in our Galactic center has an X-ray luminosity less than 5×10^{35} ergs s^{-1} and perhaps $L_X \sim 10^{35}$ ergs s^{-1} (Koyama et al. 1996) and a 20 GHz radio luminosity of $\sim 10^{34}$ ergs s^{-1}. If the black hole mass is $\sim 3 \times 10^6\ M_\odot$ (Eckart & Genzel 1996), then the observed luminosity ratio is within a factor of $\lesssim 2$ of that predicted for an ADAF source. Sgr A* and several other sources are plotted in Figure 2 along with theoretical curves of the luminosity ratio L_R/L_X. We conclude that galactic nuclei similar to ours could indeed harbor an ADAF (Narayan & Yi 1995; Narayan et al. 1997; Manmoto et al. 1997). On the other hand, extragalactic nuclei with such low luminosities would be extremely difficult to detect even if they are relatively nearby.

3.2. *NGC 4258*

For a galactic nucleus with a black hole mass $m \gtrsim 10^7$, which is often adopted for Seyferts, the ADAF mechanism implies a significantly higher radio luminosity than that of Sgr A*. Also plotted in Figure 2 is NGC 4258, which has an X-ray luminosity of $\sim 4 \times 10^{40}$ ergs s^{-1} (Makishima et al. 1994) and a black hole mass of $\sim 4 \times 10^7\ M_\odot$ (Miyoshi et al. 1995). From equation (2.10), the expected 15 GHz radio luminosity is $\sim 3 \times 10^{36}$ ergs s^{-1}. Turner & Ho (1994) report a marginally resolved, compact nuclear radio source at 15 GHz in NGC 4258. Assuming a distance of ~ 7.5 Mpc (Sandage 1996), this implies a point-source luminosity of $\lesssim 3 \times 10^{36}$ ergs s^{-1}. We conclude that it is possible that NGC 4258 is powered by an ADAF (Lasota et al. 1996).

3.3. *LINERs*

NGC 4258 belongs to a group of the emission-line galaxies known as LINERs (e.g., Osterbrock 1989). Ho et al. (1995) find that nearly one-third of all nearby galaxies with B magnitude less than or equal to 12.5 are LINERs. Moreover, a substantial fraction of them contain broad-line regions, which suggest that these sources may be powered by accretion flows similar to those in AGNs (Filippenko & Sargent 1985). On account of relatively low X-ray luminosities and hard X-ray emission, LINERs are prime candidates for ADAFs. It is, however, unclear whether the accretion occurs in the form of an ADAF or a high-efficiency accretion disk as in Seyfert galaxies (e.g., Lasota et al. 1996). Since the LINERs are classified solely based on the optical line ratios, the LINERs as a class may be highly heterogeneous. It cannot be ruled out that some of the galaxies have ADAFs and some have low-luminosity versions of the AGN accretion flows. It is tempting to speculate that the Seyfert-type LINERs could have higher X-ray luminosities but relatively lower nuclear radio luminosities than ADAF-type LINERs. In this regard, the ADAF radio/X-ray luminosity relation is particularly promising in distinguishing the X-ray emission mechanism in emission-line galaxies. For Seyferts with thin disk accretion and radio jets, the extended radio emission could be much larger than was indicated by equation (2.10).

From a cursory search of the literature we identified eight LINERs (NGC 3031, 3079, 3627, 3628, 4258, 4486, 4736, and 5194) with both measured X-ray fluxes and high angular resolution ($\sim 1''$), high-frequency ($\gtrsim 10$ GHz) radio fluxes. The ratios of radio luminosity to X-ray luminosity for these sources are plotted in Figure 2 along with ADAF curves for black hole masses ranging from 10^6 to $10^9\ M_\odot$. For two sources (NGC 3627 and 4736) we computed the 2–10 keV fluxes from the 0.5–2 keV *ROSAT* fluxes assuming an $\alpha_X = 0.6$ power law. The error in this extrapolation factor is less than 2 for a range of spectra from hard to soft. We also computed the 15 GHz radio flux of NGC 3627 from the reported 8.1 GHz flux and of NGC 4486 from the reported 22 GHz flux using the predicted $\nu^{2/5}$ power law (eq. [2.5]). The distances to these galaxies were taken from Freedman et al. (1994), Sandage (1996), Lehnert & Heckman (1995), Sandage & Tammann (1987), van den Bergh (1996), and Baan & Haschick (1983) and also have significant uncertainties. Also in Figure 2, we show the luminosity ratios of five typical radio-quiet Seyfert galaxies for comparison.

Even the $\sim 1''$ resolution is far too large to resolve the radio-emitting region of ADAFs. For example, at 10 Mpc, $1''$ corresponds to 50 pc compared with the expected $\ll 1$ pc size of the ADAF-emitting region. To the extent that there are other radio sources, e.g., H II regions or radio jets, in the radio beam, then the ratios of Figure 2 should be considered upper limits. Of course, the resolution of the X-ray observations is even worse; however, it seems unlikely that there are other X-ray sources with luminosities greater than 10^{40} ergs s^{-1} within 50 pc of the nucleus. If there are such sources, then they would have the effect of artificially lowering the luminosity ratio. Knowledge of the X-ray and radio spectra would help clarify these issues.

We caution that the list of sources is neither unbiased nor complete. We do not intend the plot to be strong evidence for the existence of the ADAF mechanism in these sources; rather we intend only for it to be suggestive that this might be the case. In any case, the uncertainty of black hole masses in these systems coupled with the strong dependence of radio luminosity on black hole mass precludes a detailed comparison of observations and predictions. Nevertheless, most of the sources in Figure 2 appear to be consistent with the predicted ADAF luminosity ratios for black hole masses $m \sim 10^7$–10^8 (NGC 3079 and NGC 4486 are separately discussed below). It is gratifying that the black hole masses are close to those often invoked for Seyfert-type AGNs (e.g., Padovani 1989).

3.4. *Seyfert Galaxies*

Low-luminosity Seyferts with $L_X \lesssim 10^{43}$ ergs s^{-1} could also be powered by ADAFs. The five examples of Seyferts shown in Figure 2 are accounted for by the ADAF emission if they contain black holes with masses $\sim 10^8$–$10^9\ M_\odot$. If their radio emission is from an ADAF, the positions of the Seyferts would imply that the sources are accreting at higher accretion rates closer to the theoretical maximum $\dot{m}_{\rm crit}$ than the LINERs shown. On the other hand, if the Seyferts contain high radiative efficiency flows, the mass-accretion rates and black hole masses could be substantially lower than those estimated in Figure 2. Then the radio emission is most likely due to a radio jetlike emission mechanism. In this case, high-resolution radio observations could reveal the radio jets. NGC 1068 and 4151 do appear to contain jetlike features (e.g., Wilson & Ulvestad 1982). NGC 1068 has a relatively strong compact nuclear radio

source at the subarcsecond scale (Gallimore et al. 1996), which results in a much higher radio/X-ray flux ratio than the rest of the Seyferts shown in Figure 2. The radio emission from an ADAF can explain such a high ratio only if $M \sim 10^9\ M_\odot$. If the black hole mass of NGC 1068 is typical of Seyferts, i.e., is less than $10^8\ M_\odot$, the relatively high radio luminosity might indicate small-scale radio jet activity. However, given the small linear scale, $\lesssim 5$ pc (Gallimore et al. 1996), radio emission from an ADAF seems more likely. If the latter is the case, then the black hole mass is estimated to be close to $\sim 10^9\ M_\odot$. It should be noted that starburst activity in NGC 1068 contributes to the nuclear, hard X-ray emission (e.g., Ueno et al. 1994). NGC 4151 is a variable X-ray source so we used the mean 2–10 keV flux (Papadakis & McHardy 1995).

3.5. *Radio Bright Sources: Need for High-Resolution Radio Observations*

The high radio to X-ray ratio of NGC 3079 also implies a black hole mass as high as $\sim 10^9\ M_\odot$. This is also the case for the giant elliptical galaxy NGC 4486 (M87). For M87 the dynamical estimates of the black hole mass, $\sim 3 \times 10^9\ M_\odot$ (Harms et al. 1994) are indeed consistent with the position of the source in Figure 2. NGC 4486 does have a radio jet; however, the radio flux quoted here is from a VLBI measurement (Moellenbrock et al. 1996) and corresponds to a spatial resolution of less than 1 pc. The similarity between the type 2 Seyfert NGC 1068 and the two LINERs NGC 3079 and 4486 is intriguing, and it may suggest a common emission mechanism in the two different types of active galaxies with comparable luminosities.

Generally, radio-loud galactic nuclei populate the upper right-hand region of Figure 2. NGC 3079, 4486, and 1068 are relatively radio loud, and so it is crucial to extract the compact nuclear radio emission (i.e., excluding the contribution from extended radio lobes). While ADAF radio sources are too small ($\ll 1$ pc) to be resolved even by VLBI or VLBA, high angular resolution observations would serve to remove contamination by extended nuclear or nonnuclear emission. Furthermore, observations at two frequencies would test whether or not the sources have the predicted inverted spectrum. Measurements of the X-ray spectral index would further test the ADAF emission mechanism.

4. GALAXIES AS A SOURCE OF THE X-RAY BACKGROUND

The cosmic XRB intensity at energy E is given by

$$\frac{dI(E)}{dE} = \frac{c}{4\pi H_0} \int_0^{z_c} dz\, \frac{j[E(1+z),\, z]}{(1+z)^2(1+\Omega_0 z)^{1/2}}\,, \qquad (4.1)$$

where Ω_0 is the usual cosmological density parameter, $j(E, z)$ is the comoving volume emissivity, and $H_0 = 100\ h$ km s^{-1} Mpc^{-1} is the Hubble constant. For discrete sources with individual differential luminosity dL/dE and comoving number density n, $j[E(1+z),\, z] = n(z) dL/dE(z)|_{E(1+z)}$. We assume that the sources exist up to redshift $z = z_c$. If the emissivity evolution is driven by the pure luminosity evolution (i.e., without significant spectral or number density evolution), one can roughly estimate the number density required to account for the observed XRB. For pure luminosity evolution of the form $L \propto (1+z)^K$ and a power-law spectrum $dL/dE \propto E^{-\alpha_X}$, the integrated XRB between the energies E_1 and E_2 is

$$I_{\rm XRB} = \int_{E_1}^{E_2} dE\, \frac{dI}{dE} = \frac{cnL_{12}}{2\pi H_0 (2K - 2\alpha_X - 3)} \times [(1+z_c)^{K-\alpha_X-3/2} - 1]\,, \qquad (4.2)$$

where $L_{12} = \int_{E_1}^{E_2} dE (dL/dE)$ and $\Omega_0 = 1$ have been assumed for simplicity. Therefore,

$$nL_{12} = \frac{2\pi H_0\, I_{\rm XRB}(2K - 2\alpha_X - 3)}{c} \times [(1+z_c)^{K-\alpha_X-3/2} - 1]^{-1}\,. \qquad (4.3)$$

The observed XRB is fitted by (e.g., Gruber 1992)

$$\frac{dI}{dE} = 7.877 \left(\frac{E}{1\ \text{keV}}\right)^{-0.29} \exp\left(\frac{-E}{41.13\ \text{keV}}\right) \times \text{keV s}^{-1}\ \text{cm}^{-2}\ \text{sr}^{-1}\ \text{keV}^{-1}\,, \qquad (4.4)$$

and, therefore, $I_{\rm XRB} \approx 30$ keV s^{-1}cm^{-2}sr^{-1} for $E_1 = 2$ keV and $E_2 = 10$ keV. If $K = 3$ and $z_c = 2$ (e.g., Almaini et al. 1997), with $\alpha_X = 0.4$ and $h = 0.65$, then $nL_{12} \sim 6 \times 10^{38}$ ergs s^{-1} Mpc^{-3}, which is consistent with the local X-ray emissivity measured by Miyaji et al. (1994). To account for 50% of the 2–10 keV XRB in terms of low-luminosity ($L_X \sim 10^{41}$ ergs s^{-1}) sources requires a comoving number density of $n \sim 3 \times 10^{-3}$ Mpc^{-3}, which is comparable to the density of L^* galaxies (e.g., Peebles 1993).

5. SUMMARY AND DISCUSSION

Recent developments in the study of the XRB indicate the necessity of relatively faint, hard-spectrum X-ray sources. These sources could be either heavily obscured low-luminosity AGNs or X-ray–bright emission-line galaxies. The implied luminosity of these X-ray–bright galaxies is similar to that of LINERs and other narrow emission line galaxies, and it has been suggested that nearly one-third of all nearby galaxies are LINERs (Ho et al. 1995). A prime candidate for the emission mechanism of X-ray–bright galaxies is ADAF onto a central, massive black hole. While classical bright AGNs are expected to have weak radio emission (unless they have radio jets), ADAF sources exhibit high-frequency radio emission from a hot synchrotron-emitting plasma. The radio luminosities of ADAFs are modest (observations at 20 GHz would only be able to detect them to distances of $\lesssim 30$ Mpc); however, the characteristic inverted radio spectrum provides an observational test for the ADAF paradigm. If ADAFs are unambiguously detected, the radio/X-ray luminosity relation provides a direct estimate of the central black hole mass. Several nearby LINERs have radio to X-ray luminosity ratios that are consistent with the ADAF predictions; however, more observations are needed to test the predictions presented in this paper.

An important consequence of the inherently inefficient ADAF mechanism is the implied growth rate for the masses of the central black holes. If a typical source of 2–10 keV luminosity at $z = 0$ is $L_X \sim 10^{41}$ ergs s^{-1}, and if the sources undergo the luminosity evolution of the form $(1+z)^3$ up to redshift 2 (as suggested by Almaini et al. 1997), then at $z = 2$, the source has a luminosity of $\sim 3 \times 10^{42}$ ergs s^{-1}, which is similar to the luminosities of some X-ray–bright galaxies (Griffiths et al. 1996 and references therein). The

approximate minimum black hole mass for these sources consistent with ADAF emission can be estimated by equating this luminosity with the maximum bremsstrahlung luminosity expected from the ADAF accretion flow. The maximum 2–10 keV band limited flux is $\sim 10^{42} m_7$ ergs s^{-1} (Narayan & Yi 1995). Then the minimum black hole mass at $z = 2$ is $\sim 3 \times 10^7\ M_\odot$. An estimate of the current black hole mass for these sources at $z = 0$ is obtained by assuming that these sources continue to accrete at a rate of $\dot{m} \sim \dot{m}_{\rm crit} \sim 2 \times 10^{-2}$ from $z = 2$ to $z = 0$ (cf. Yi 1996). The resulting black hole mass, $\sim 5 \times 10^7\ M_\odot$, is similar to the typical black hole mass assumed for Seyfert galaxies and the black hole mass observed in NGC 4258. This rough estimate is not intended to be a prediction of the current mass spectrum of galactic black holes but rather to check whether or not the ADAF mechanism violates current estimates of central black hole masses.

We have hypothesized that ADAFs around central black holes in galaxies generate a substantial component of the hard XRB. This requires that a significant fraction of galaxies harbor central black holes with ADAF flows. However, even if the number density of ADAF sources is too small to contribute significantly to the XRB (cf. Di Matteo & Fabian 1997), ADAFs are still interesting for X-ray–bright emission-line galaxies, and the observational tests suggested here are useful probes of the X-ray emission mechanism.

We would like to thank Ramesh Narayan for information on the spectral states of accreting black holes and Roeland van der Marel for helpful discussions on black hole masses. This work was supported in part by the SUAM and Monell Foundations and NASA grant NAG 5-3015.

REFERENCES

Almaini, O., Shanks, T., Griffiths, R. E., Boyle, B. J., Roche, N., Georgantopoulos, I., & Stewart, G. C. 1997, MNRAS, 291, 372
Bann, W. A., & Haschick, A. D. 1983, AJ, 88, 1088
Beckert, T., & Duschl, W. J. 1997, A&A, 328, 95
Boyle, B. J., Shanks, T., Georgantopoulos, I., Stewart, G. C., & Griffiths, R. E. 1994, MNRAS, 271, 639
Brinkmann, W., Siebert, J., & Boller, Th. 1994, A&A, 281, 355
Carral, P., Turner, J. L., & Ho, P. T. P. 1990, ApJ, 362, 434
Comastri, A., et al. 1992, ApJ, 384, 62
Della-Ceca, R., et al. 1996, ApJ, 469, 662
Di Matteo, T., & Fabian, A. C. 1997, MNRAS, 286, 393
Eckart, A., & Genzel, R. 1996, Nature, 383, 415
Fabbiano, G. 1989, ARA&A, 27, 87
Fabbiano, G., Kim, D. W., & Trinchieri, G. 1992, ApJS, 80, 531
Falcke, H., Wilson, A. S., & Ho, L. C. 1997, preprint (astro-ph/9708126)
Filippenko, A. V., & Sargent, W. A. 1985, ApJS, 57, 503
Frank, J., King, A. R., & Raine, D. 1992, Accretion Power in Astrophysics (Cambridge: Cambridge Univ. Press)
Freedman, W. L., et al. 1994, ApJ, 427, 628
Gallimore, J. F., et al. 1996, ApJ, 458, 136
Gendreau, K. C., et al. 1995, PASJ, 47, L5
Georgantopoulos, I., et al. 1993, MNRAS, 262, 619
———. 1996, MNRAS, 280, 276
Ghisellini, G., Haardt, F., & Matt, G. 1994, MNRAS, 267, 743
Griffiths, R. E., Della-Cella, R., Georgantopoulos, I., Boyle, B. J., Stewart, G. C., Shanks, T., & Fruscione, A. 1996, MNRAS, 281, 71
Gruber, D. E. 1992, in The X-Ray Background, ed. X. Barcons & A. C. Fabian (Cambridge: Cambridge Univ. Press), 44
Harms, S. N., et al. 1994, ApJ, 435, 35
Hasinger, G., et al. 1993, A&A, 275, 1
Hasinger, G., Burg, R., Giacconi, R., Schmidt, M., Trumper, J., & Zamorani, G. 1997, A&A, 329, 482
Ho, L. C., Filippenko, A. V., & Sargent, W. A. 1995, ApJS, 98, 477
Koyama, K., Maeda, Y., Sonobe, T., Takeshima, T., Tanaka, Y., & Yamauchi, S. 1996, PASJ, 48, 249
Lasota, J.-P., et al. 1996, ApJ, 462, 142
Lehnert, M. D., & Heckman, T. M. 1995, ApJS, 97, 89
Mahadevan, R. 1996, ApJ, 465, 327
Makishima, K., et al. 1994, PASJ, 46, L77
Manmoto, T., Mineshige, S., & Kusunose, M. 1997, ApJ, 489, 791
Miyaji, T., et al. 1994, ApJ, 393, 134
Miyoshi, M., et al. 1995, Nature, 373, 127
Moellenbrock, G. A., et al. 1996, AJ, 111, 2175
Narayan, R., & Yi, I. 1995, ApJ, 444, 231
Narayan, R., Yi, I., & Mahadevan, R. 1995, Nature, 374, 623
Narayan, R., Mahadevan, R., Grindlay, J. E., Popham, R. G., & Gammie, C. 1998, ApJ, 492, 554
Osterbrock, D. E. 1989, Astrophysics of Gaseous Nebulae and Active Galactic Nuclei (Mill Valley: University Science Books)
Padovani, P. 1989, A&A, 209, 27
Papadakis, I. E., & McHardy, I. M. 1995, MNRAS, 273, 923
Peebles, P. J. E. 1993, Principles of Physical Cosmology (Princeton: Princeton Univ. Press), 122
Rees, M. J., Begelman, M. C., Blandford, R. D., & Phinney, E. S. 1982, Nature, 295, 17
Reynolds, C. S., et al. 1996, MNRAS, 283, 111
Saikia, D. J., Pedlar, S. W., Unger, S. W., & Axon, D. J. 1994, MNRAS, 270, 46
Sandage, A. 1996, AJ, 111, 18.
Sandage, A., & Tammann, G. A. 1997, A Revised Shapley-Ames Catalogue of Bright Galaxies (2d ed.; Washington, DC: Carnegie Institute)
Schmidt, M., et al. 1998, A&A, 329, 495
Serlemitsos, P., Ptak, A., & Yaqoob, T. 1997, preprint (astro-ph/9701127)
Smith, D. A., & Done, C. 1996, MNRAS, 280, 355
Soltan, A., & Hasinger, G. 1994, A&A, 288, 77
Spencer, R. E., & Junor, W. 1986, Nature, 321, 753
Turner, J. L., & Ho, P. T. P. 1994, ApJ, 421, 122
Ueno, S., et al. 1994, PASJ, 46, L71
van den Bergh, S. 1996, PASP, 108, 109
Wilson, A. S., & Ulvestad, J. S. 1982, ApJ, 263, 576
Yi, I. 1996, ApJ, 473, 645